AIAA-99-0534

TAKEOFF/LANDING ASSESSMENT OF AN HSCT WITH PNEUMATIC LIFT AUGMENTATION

Dimitri N. Mavris[†] and Michelle R. Kirby[‡]

Aerospace System Design Laboratory (ASDL)
School of Aerospace Engineering
Georgia Institute of Technology
Atlanta, GA 30332-0150

ABSTRACT

Pneumatic technologies, such as Circulation Control airfoils, have been experimentally demonstrated to generate very high lift coefficients at low angles of attack. These blown airfoils offer great potential for advanced subsonic transports. Yet, the potential of this particular pneumatic technology is not limited to subsonic aircraft. In fact, Circulation Control has been chosen as an enabling technology to be applied on a generic High Speed Civil Transport (HSCT) under NASA Grant NAG-1-1517. Research on this contract was directed to a first-order quantitative estimate of the impact of Circulation Control on the takeoff and landing performance of an HSCT and is summarized in this paper. A reference point was established with an HSCT utilizing conventional high-lift devices that resulted in a takeoff field length of approximately 13,000 ft. The incremental changes in lift and drag established from the wind tunnel experiments performed in the above stated grant were then applied to this configuration and the low speed performance enhancements and degradations were quantified. The application of Circulation Control was shown to reduce the takeoff field length by as much as 31% from the reference point. This result strongly warrants further investigations with higher order analysis since the first order estimate shows significant improvements in low speed performance of an HSCT with Circulation Control pneumatic technology.

INTRODUCTION

Travelers have always welcomed the idea of reaching distant destinations in less time without having to spend a great deal of money. Over the last 60 years, this demand has driven the need for commercial aircraft that can fly farther and faster than those of previous generations. Passenger travel started with the Ford Tri-motor, progressed through propeller driven aircraft, such as the Douglas DC-3, to turbojet powered aircraft such as the Boeing 707. Today, passenger aircraft are powered by high bypass turbofan engines such as those on the Boeing 777. However, with the exception of the Concorde, the speed of commercial aircraft has not significantly increased over the last 20 years because of the enormous technical difficulties associated with faster-than-sound travel in an economically viable manner. However, the technology to achieve faster-than-sound commercial travel in an economically viable manner has matured to the point that full-scale application may be possible. A High Speed Civil Transport (HSCT) in the United States and the Second Generation Supersonic Transport Initiative in Europe are the only current, active candidates to replace the aging Concorde.

High Speed Civil Transport

The greatest challenge facing an HSCT is the necessity to go farther and faster with a greater payload capacity than the Concorde at an operating cost for the airlines comparable to that of current subsonic transports. This translates to an increase in vehicle range and passenger capacity while minimizing the fuel cost per trip. Furthermore, recent studies have revealed that the success of an HSCT will require significant technological advances in order to provide the environmental compliance, airport compatibility, and economic viability.[1,2]

Based on the current NASA High Speed Research program effort, an HSCT is a Mach 2.4, 300 passenger aircraft with a 5,000 nm range[3] and four mixed-flow turbofan (MFTF) engines.[4] The aircraft is restricted to subsonic flight over land due to the impact of sonic boom, and it must abide by all FAA regulations. Previous studies have shown that an HSCT is not

[†] Asst. Professor, School of AE, AIAA Senior Member
[‡] Graduate Research Asst., AIAA Student Member
Paper presented at the 37th Aerospace Sciences Meeting & Exhibit, Reno, NV, January 11-14, 1999

technically feasible or economically viable with conventional technologies.[2,5,6,7] Feasibility and viability are measured by compliance with noise levels, takeoff and landing field length requirements, gross weight limitations, and affordability goals. Various technologies have been proposed to address these issues including composite materials to reduce weights,[5,8] advanced engines to reduce SFC,[4,5,6] laminar flow devices to reduce cruise drag,[5] and Circulation Control to improve low speed characteristics.[9] The application of Circulation Control to an HSCT will be the focus of this study.

Circulation Control

Circulation Control (CC) is considered one of the most efficient methods for lift augmentation at low speed flight.[10] CC augments an airfoil's lift capability by tangentially ejecting a thin jet of high momentum air over a rounded trailing edge, as shown in Figure 1.[11] Provided its velocity is greater than the local outer flow, the jet sheet will remain attached over the curved surface by means of the Coanda effect.[12,13,14] This behavior arises from the low pressure region created by the jet which energizes the boundary layer across the mixing boundary. The suction created by the low pressure region is sufficient to overcome the centrifugal forces and remains attached onto the lower surface of the airfoil. The trailing edge stagnation point moves to the lower surface, thereby increasing the airfoil circulation, and hence, the lift.[15] The characteristic parameter which describes the amount of energy injected into the flow is the blowing coefficient, C_μ. The blowing coefficient is proportional to the ejected mass flux, $\dot{m}_j$, and jet velocity, V_j, and inversely proportional to the freestream dynamic pressure, q_∞, and the wing reference area, S_{ref}. Typical trends in force coefficient augmentation include an increase in lift and drag with increasing C_μ as will be shown later.

The characteristic of a wall jet remaining attached to a curved surface dates back to 1800 when Young first described the phenomena[12] and later to Henri Coanda in 1910.[13,14] Yet, the CC concept was not seriously investigated until the early 1960's by Dunham[16] and later Cheeseman,[17] both of the National Gas Turbine Establishment in England. Dunham focused on application of CC to circular cylinders and Cheeseman on the development of CC airfoils for rotorcraft. In the late 1960's, work first began in the United States at the David Taylor Model Basin.[18,19] Most CC research efforts have focused on the application to rotorcraft and/or short takeoff and landing (STOL) vehicles where an elliptical, or rounded trailing edge, airfoil was used (Figure 1).

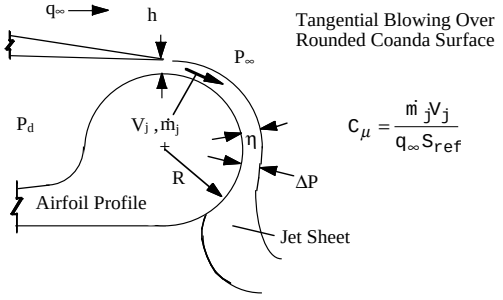

Figure 1: Circulation Control Aerodynamic Features

The CC concept was first demonstrated at West Virginia University in April 1974 on the WVU CC Technology Demonstrator STOL[20] and five years later in 1979 on a modified Navy Grumman A-6A.[21,22] The purpose of these flight tests was to demonstrate the advantages which had been proposed by the application of CC. In particular, the advantages included reduction in landing velocities, increased aircraft payload and wing loading, high drag generation on approach, reduced landing and takeoff distances, and improved pilot visibility.[11] Both of these demonstrators had rounded trailing edge sections to maximize the Coanda effect. Yet, the blunt trailing edges tended to negatively affect other characteristics of flight and performance of the aircraft. For example, the blunt trailing edge increased the drag during cruise due to premature flow separation, and the parasitic drag increased due to energy requirements to provide the blowing, and large negative pitching moments resulted from large suction peaks on the upper surface trailing edge regions.[23] These problems could be overcome by applying a sharp trailing edge,[24] a splitter plate,[23] or a dual-radius circulation control wing (CCW) concept.[25] The CCW, shown in Figure 2, relieved the high drag associated with the mixing of the blown air and freestream and the separation of the blown air on the lower surface.[24]

The development of the CCW has been a primary focus of recent experimental investigations. The dual-radius CC airfoil was initially applied to a modified Boeing 737-200[25] and more recently to an HSCT-type aircraft.[26] The wind tunnel data from these experiments will be utilized for this paper on a full size notional HSCT configuration.

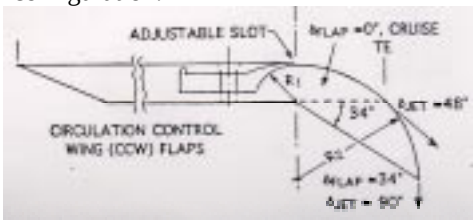

Figure 2: Dual-radius CC Airfoil Concept[26]

METHODOLOGY

The primary aspiration of the current investigation was to objectively assess the feasibility of the application of a low speed pneumatic technology, in particular CC, to an HSCT concept. This technology has been proven for various subsonic vehicles including a Grumman A-6 and a Boeing 737. Its potential has been extensively investigated for decades in wind tunnels across the globe for application to rotorcraft. More recently, an experimental investigation was performed at the Georgia Tech Research Institute (GTRI) with application to an HSCT-type configuration as described in Reference 26. The data from those experiments was applied to a full scale computational model so as to assess, with a first order estimate, the impact of CC from a system level point of view. This objective was achieved in three steps:

- Defining the need
- Wind tunnel data reduction
- Performance assessment

Defining the Need

Up to this point, a qualitative justification of the need for CC on an HSCT was inferred, but a quantitative assessment was desired. This assessment was facilitated by the Technology Identification, Evaluation, and Selection (TIES) method developed at the Aerospace Systems Design Laboratory (ASDL).[2] The TIES seven-step process provides a decision maker/designer with an ability to easily assess, identify, and trade-off the impact and/or need of various technologies in the absence of sophisticated, time-consuming mathematical formulations. The seven steps include problem definition, baseline and alternative concepts identification, modeling and simulation, design space exploration, determination of system feasibility (probability of success), population of the pugh evaluation matrix, and best alternative concept determination. The result of the application of the TIES method quantitatively established the need for low speed lift augmentation of a HSCT due to violation of performance constraints. Hence, if a particular technology could be applied to an HSCT which could physically provide the needed improvements predicted by the TIES method, the HSCT could become a technically feasible concept. The next two steps offer a solution to obtain feasibility through the application of Circulation Control.

Wind Tunnel Data

Once the need for CC was established, the application of the technology to a conventional configuration was desired. To implement this step, trends associated with various C_μ levels, flap settings, and angle of attack, α, were needed. This assessment entailed a reduction of the wind tunnel data from experiments performed by Mr. Bob Englar at GTRI. The test model was an existing GTRI half-span model and the wing planform was representative of a generic HSCT as seen in Figure 3. The fuselage was a typical National Aerospace Plane (NASP) model and the wing planform was a low aspect ratio double-delta with leading edge sweeps of 75° and 54°. The wing sections employed a quarter inch flat plate with a sharply-beveled leading edge and a dual radius trailing edge flap as shown in Figure 2. Two horizontal tails, two canards, and a NASP-type vertical tail were also used in the wind tunnel experiments. A variety of experiments were performed on this model including: with and without canards, with and without horizontal and vertical tails, various blowing levels, angle of attack (α) sweeps, various flap types (CCW flap and blown jet flap), flap settings, and different slot heights. Wind tunnel runs with the horizontal and vertical tails and canards were neglected. The rationale behind this decision was to isolate the effects of CC on the wing. Furthermore, the CCW flap (Figure 2) runs were considered to be more applicable than the blown jet flap due to greater lift augmentation capability. The data provided to the authors included lift and drag coefficients as a function of α, C_μ, and flap settings for a fixed dynamic pressure. Once the relevant data set was identified, it was reduced to an appropriate form for the low speed performance code described below.

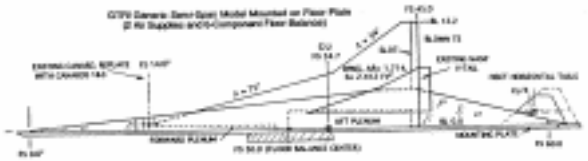

Figure 3: GTRI Experimental Generic HSCT Model[26]

Performance Assessment

The performance assessment of an HSCT utilizing the CC technology was performed in three steps. First, a reference point was established for the low-speed metrics (takeoff field length, rotation speed, etc.) of a configuration which utilized only conventional high-lift systems, such as Krueger flaps. Second, the trends established from the wind tunnel experiments were applied to a full-scale configuration. And finally, the CC impact was quantified.

The takeoff and landing quantitative performance assessments were based on an analysis of a representative configuration using the NASA Langley developed program, TAKEOFF Version 2.0.[27]

TAKEOFF is a stand-alone version of the FLight OPtimization System[28] (FLOPS) takeoff and landing module. The TAKEOFF program was based on an analysis of a commercial vehicle's low speed performance such that all applicable FAR 25 regulations were met. All FAR requirements were determined including second-segment climb gradient, missed approach climb gradient, constrained speeds for all engines operating (AEO) and one engine inoperative (OEI) conditions, etc. Furthermore, the balanced field length was calculated based on FAR 25 requirements. A typical takeoff profile is shown in Figure 4 with the low speed metrics of interest for the current investigation. The metrics included the balanced takeoff field length (TOFL), stall speed (V_S), decision speed (V_1), rotation speed (V_R), liftoff speed (V_{LOF}), and obstacle height speed (V_2).

The TAKEOFF program required, at a minimum, the following input parameters to determine the low speed performance metrics: takeoff gross weight, maximum landing weight, wing area, atmospheric temperature, altitude, engine performance characteristics, maximum C_L for takeoff and landing, and arrays of C_L and C_D, both as functions of α, for takeoff and landing. All performance assessments assumed in-ground-effect.

The OEI condition was of primary importance for the current investigation since the application of the CC technology is dependent upon the ejected mass flux which was supplied from the engines. Hence, if the OEI condition occurs, not only does the thrust reduce, the freestream dynamic pressure reduces *and* the amount of bleed flow reduces. From the definition of the blowing coefficient given in Figure 1, if the mass flux reduces due to less bleed supply from OEI, the blowing coefficient reduces and the incremental change in the force coefficients (C_L and C_D) also decrease. Therefore, in addition to the low speed metrics, an issue to be addressed was the low speed performance degradation due to OEI or possible engine oversizing.

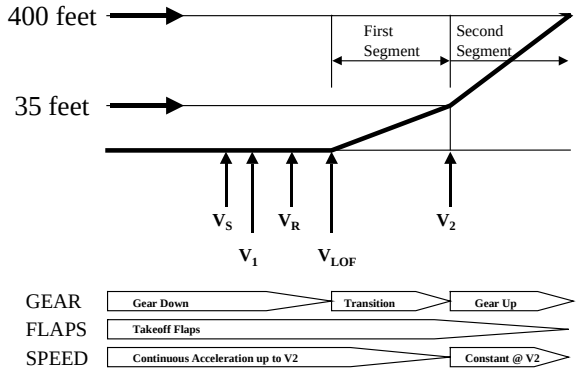

Figure 4: Typical Takeoff Profile

IMPLEMENTATION

Defining the Need

A design space investigation was performed on an HSCT via the TIES method. Subsequently, the need for CC was established. The details of this investigation are provided in Reference 2, and the information relevant to the current research is summarized below. First, the design space exploration of a conventional technology concept was defined by parameters such as wing area and geometry, wing thickness-to-chord ratios, thrust-to-weight ratio, engine cycle parameters, etc. The design space system feasibility was constrained by the parameters listed in Table I.

Based on these constraints, the system feasibility of a conventional design space was established based on the probability of success. The probability of success is analogous to the percentage of the defined design space which satisfies the imposed constraints. The probability of success was shown to be satisfactory for landing field length (95.1%) and takeoff gross weight (84.1%). Yet, the remaining four constraints had unacceptable probability levels: V_{app} (20.1%), flyover noise (13.7%), sideline noise (0%), and takeoff field length (35.8%). Since the probability of success was low, the TIES method suggested the infusion of new technologies. An initial estimate of the impact of new technologies was achieved through Technology Impact Forecasting (TIF). The reader is referred to References 29 and 30 for more detailed information on this method. One key technology which was shown to improve the low speed metrics was CC. Yet, at the time of that investigation, CC was simulated through a 30% increase in C_{Lmax} to provide initial insight and establish the need. Yet, the current research was focused on confirming that the 30% increase in C_{Lmax} was physically realizable with circulation control. The remainder of this study investigated, in detail, the low speed performance of a notional HSCT utilizing actual wind tunnel experimental data trends.

Table I: HSCT Performance Constraints

Parameter	Target/ Constraint	Units
Performance		
Approach Speed (V_{app})	Š 155	kts
FAR 36 Stage III Flyover Noise (FON)	Š 106	EPNLdB
Landing Field Length (Landing FL)	Š 11,000	ft
FAR 36 Stage III Sideline Noise (SLN)	Š 103	EPNLdB
Takeoff Field Length (TOFL)	Š 11,000	ft
Takeoff Gross Weight (TOGW)	Š 1,000,000	lbs

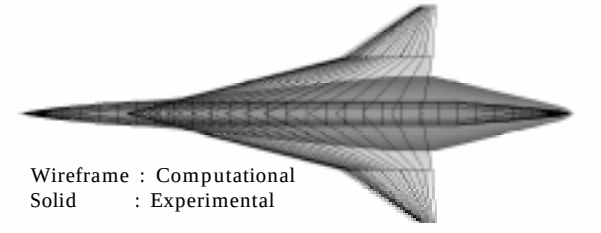

Figure 5: HSCT Model Comparison

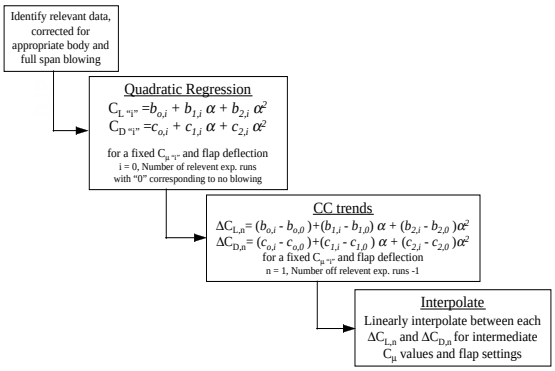

Figure 6: Wind Tunnel Data Reduction Schematic

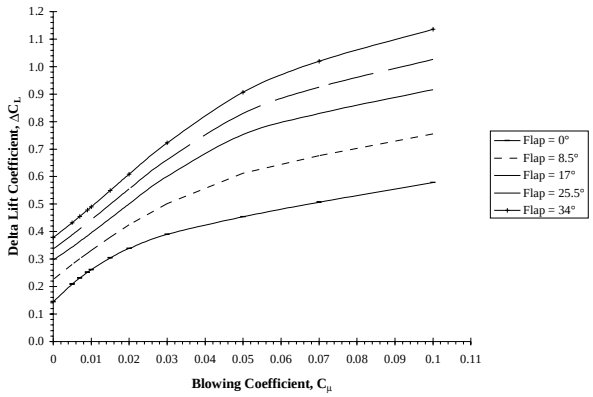

Figure 7: "Corrected" Incremental C_L Trends (α=0º)

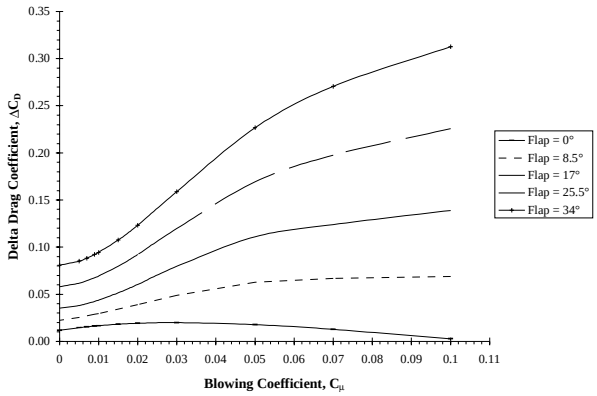

Figure 8: "Corrected" Incremental C_D Trends (α=0º)

Wind Tunnel Data

As stated previously, data was supplied to the authors in the form of C_L and C_D as functions of α, C_μ, and flap settings for the model shown in Figure 3. Yet, the flat plate model was not a realistic design for assessing the performance impact of CC on a full scale configuration. A scaled wing utilizing the airfoil shown in Figure 2 would have minimal wing thickness available for fuel storage and would be aerodynamically inefficient without twist or camber. Additionally, the fuselage was not realistic for an HSCT-type vehicle. Therefore, an adaptation of the wind tunnel model was generated. The original wing planform was maintained but the wing was given a constant 4% thickness-to-chord ratio. Based on previous studies performed by the authors, the wing was twisted and cambered for a top of climb lift coefficient of 0.1. The NASP fuselage utilized in the experiments was converted to a slender body (maximum diameter of 16.0 ft) and shaped based on an internal layout assessment for a tri-class 300 passenger arrangement. Once the wing was twisted and cambered for the cruise lift coefficient, the wing planform changed slightly. An overlay of the computational model (wireframe) and experimental model (shaded) is shown in Figure 5.

Empirical corrections to the wind tunnel data were performed by GTRI to correspond to the computational geometry. These corrections included consideration of a larger exposed trailing edge for more spanwise blowing and lower drag associated with the slender body. Based on the force coefficients provided, a more useful form of the data was needed to conduct the performance assessment. In particular, the TAKEOFF program required that an incremental change in C_L or C_D was represented as a function of vehicle speed for a fixed flap setting and fixed α. The dependency of the force coefficients on speed for the TAKEOFF program assumed that the incremental change of forces coefficients *were constant* with speed. This created difficulty in the performance assessment, as will be discussed, since the blowing coefficient was dependent upon the dynamic pressure (vehicle speed). Based on this requirement, the "corrected" data was manipulated and reduced as shown in Figure 6. With the aid of a statistical package, JMP,[31] the "corrected" data was regressed as a quadratic polynomial for each C_μ and flap setting so that an incremental change in lift and drag could be obtained. The "corrected" incremental change in the force coefficients as a function of blowing level and flap setting are shown in Figure 7 and Figure 8 for an α of 0º. Other angle of attack settings were omitted here for brevity.

At the no blowing condition, C_μ=0, there existed a finite incremental change in C_L (Figure 7) and C_D (Figure 8). This was due to the added curvature of the CCW flap (Figure 2) as compared to conventional mechanical flaps, even in the retracted position. The curvature of the CCW flaps adds more effective camber to the wing, and thus more C_L and C_D. The reader is referred to Reference 25 for more information on this phenomena. It should be noted that for increasing α, both C_L and C_D increase linearly up to stall.[26]

Performance Assessment

The conventional configurations considered in the design space exploration obtained lift augmentation by leading edge vortex generation caused by the highly swept wings. Since the highly swept wing was designed for supersonic cruise, the low speed performance was compromised. Hence, lift augmentation and high angles attack are required to achieve high lift at takeoff and landing to meet field length requirements. The angle of attack requirement could lead to exotic and costly features such as fuselage nose droop and/or synthetic vision which add weight and complexity to the entire system. Furthermore, the low speed performance was further compromised by operational constraints. For example, at rotation, the angle of attack is limited to 9.8º due to tail strike. And, after lift off, the angle of attack can be no greater than 20º due to passenger comfort and FAR requirements. To fulfill the objectives of this study, these considerations were taken into account while assessing the low speed metrics. Moreover, since 95.1% of the design space investigated could satisfy the landing field length requirement of 11,0000 ft, only the TOFL was considered for further investigation. Based on these considerations, a reference point was established for comparison. From this baseline, the CC effects were added and a one-to-one comparison ensued. The following sections describe each of these steps.

Establish Baseline

A baseline computational model was created to mimic the wing planform geometry of the wind tunnel model so that upon application of the CC trends established previously, consistency was maintained. Based on the required inputs to TAKEOFF, the baseline model was sized for a 5,000 nm mission in the sizing and synthesis code, FLOPS. The mission flown consisted of a primary cruise altitude of 67,000 ft at Mach 2.4. A subsonic cruise portion preceded the primary cruise segment at an altitude of 35,000 ft at Mach 0.9. The payload was 300 passengers with baggage, 2 flight crew, and 9 flight attendants. The experimental wing planform was scaled to 8,000 ft^2 with an aspect ratio of 2.366 in addition to the previously defined parameters. The propulsion system consisted of four MFTF engines for a 65,000 lb thrust class (sea level static). Each engine was a dual-spool co-rotating design with a 3x5 compression system and with a 1x2 turbine system. The engines were sized for a Mach 2.4 top-of-climb flight condition and the cycle was tailored for an 80%/20% super/subsonic split mission. The cycle design parameters included fan pressure ratio of 3.7, overall pressure ratio of 20, bypass ratio (BPR) of 0.7, and maximum turbine inlet temperature (T4) of 3,500 ºR. The sized configuration resulted in a takeoff gross weight of 846,908 lbs, scaled engine thrust of 67,043 lbs, and a maximum C_L at takeoff of 1.1. Additional inputs to TAKEOFF were established from internal layout designs, volume requirements, and fuselage tailoring. These inputs included a wing height of 17 ft, thrust incidence of 3º, maximum α at rotation of 9.8º, and maximum α after liftoff of 20º.

The assessment of a conventional configuration low speed performance required arrays of C_L and C_D as a function of α. A parametric variation of leading edge slats (0º to 40º) and trailing edge flap (0º to 40º) deflections was performed to obtain the optimal C_L and C_D arrays which minimized the takeoff field length (TOFL). The arrays of C_L and C_D were generated with a NASA Langley developed low speed aerodynamic code, AERO2S.[32] These arrays were inserted into TAKEOFF and the low speed metrics evaluated. The optimal settings which resulted were 0º leading edge slats and 30º trailing edge flap deflection for the following metric values: TOFL of 12,934 ft, V_S of 172.9 kts, V_1 of 186.8 kts ,V_R of 221.3 kts, V_{LOF} of 236.1 kts, and V_2 of 241 kts. These metric values were based on ideal operating conditions (e.g., standard day, maximum capacity).

A parametric study was performed on the baseline model to simulate non-ideal conditions. The parameters altered are listed in Table II. The thrust-to-weight ratio (T/W) and wing loading (W/S) were included to simulate the impact of short runways and less than full capacity conditions. The maximum lift coefficient (C_{Lmax}) was included to allow for variation in the high lift design. The rotation angle (α_{ROT}), altitude, and change in standard day temperature (in ºC) were varied for deviations in takeoff trajectory, airport altitude, and weather changes.

A Design of Experiments[33] was employed with the aid of JMP to determine the sensitivity of the low speed metrics to the parameters in Table II. The sensitivities which resulted are displayed in Figure 9 in the form of a prediction profile. The prediction profile was evaluated

Table II: Low Speed Design and Operational Parameters

Parameter	Minimum	Maximum	Unit
Thrust-to-Weight (T/W)	0.28	0.32	~
Wing loading (W/S)	95	105	lb/ft^2
CLmax	1.1	1.6	~
Rotation angle (α_{ROT})	8	12	º
Altitude	0	5,000	ft
Temperature deviation (Delta Temp)	0	16	ºC

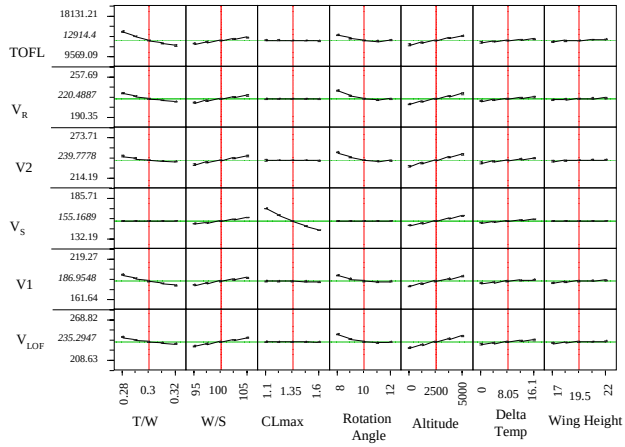

Figure 9: Conventional HSCT Configuration

based on the magnitude and direction of the slope. The larger the slope, the greater the influence of the given parameter. If a parameter, listed on the abscissa, did not contribute significantly to the response listed on the ordinate, the slope was approximately zero. The sign of the slope, either positive or negative, depicted the direction of influence of the parameter on the response. Furthermore, the limits of the metrics could be readily obtained, for example, the TOFL varied between 9,569 ft and 18,131 ft and the V_{LOF} varied between 208.6 kts and 268.8 kts. Even though the baseline configuration TOFL was improved from 12,934 ft to 9,569 ft (which satisfies the imposed constraint), this value was only achieved with a T/W of 0.32, W/S of 95 lb/ft^2, C_{Lmax} of 1.1, and α_{ROT} of 12º at standard conditions. The high value of T/W and low value of W/S implied that the passenger capacity would be low. This fact could have a detrimental impact on the HSCT economic viability.

CC Configuration

With the reference point established, the next step was to apply the force coefficient trends from the wind tunnel experiments. Yet, in order for CC to be successfully applied to an HSCT, it had to demonstrate significant performance improvements without seriously degrading the performance of other vehicle systems, particularly the engines. As stated previously, the mass flux required for lift augmentation during takeoff was assumed to be supplied from the four MFTF engine. Hence, before a low speed performance analysis was conducted, a propulsion impact assessment was investigated. Specifically, the location of extracted bleed flow was determined. Two potential extraction points were considered: fan duct and compressor discharge.

First, the case of extracting bleed flow from the fan duct was considered. Since thrust was dependent on the pressure, temperature, and mass flow at the nozzle, a decrease in fan flow due to bleed would decrease the thrust via loss in mass flow rate, but would not impact either temperature or pressure at the turbine. Therefore, the cycle specific thrust was unaffected by fan bleed. A good first order estimate of the loss in thrust due to bleed was to multiply the bleed flow by the cycle specific thrust at that flight condition and power setting to get the decrement in thrust. Since the dry specific thrust of the current engine was 98 lbf/lbm/s, bleeding 1 lbm/sec fan flow resulted in a reduction of 98 lb of net thrust. Note, this was an approximation, therefore, accuracy could become increasingly dubious as the fraction of flow bleed becomes large.

Next, the case of bleeding compressor discharge air to drive the CC system was considered. At low power, considerable excess capacity existed in the engine. Hence, the engines could be capable of providing significant flow rates of compressor discharge air during flight idle (FI) operation. The extraction of compressor discharge air would likely require an increase in T4 to maintain minimum core speed which would also increase the tailpipe temperature. Thus, the FI thrust could increase due to the compressor bleed. At high power settings (i.e., full throttle takeoff) compressor discharge bleed would result in a decrease of thrust, though not as much as that due to fan bleed. At first glance, this statement seems counter-intuitive, but was easily explained.

Consider an HSCT engine operating at full throttle SLS conditions with zero compressor bleed (i.e., cycle design point conditions). If one were to suddenly start bleeding the compressor discharge air with no change in fuel flow rate, the high pressure (HP) and low pressure (LP) spools would slow down due to a loss in core power output. As the LP spool slows, FPR drops and the specific thrust decreases, thus resulting in a "snowballing" effect where tail pipe mass flow rate, temperature, and pressure drop. Thus, thrust and specific thrust decrease, incurring a double penalty where takeoff net thrust was lost due to loss of specific thrust and loss of tailpipe mass flow rate.

Fortunately, the HSCT engine was a special case where thrust loss due to compressor bleed could be avoided if the system was properly designed. Since an HSCT engine was designed for operation at high temperature flight conditions, it would demand a high throttle ratio cycle. As a result, the core was oversized for SLS operation, and the turbine inlet temperature (T4) required to maintain 100% corrected fan speed was less than the maximum allowable. The excess T4 capacity could be used to compensate for the compressor discharge pressure (CDP) bleed by raising T4 to hold fan speed, even at high CDP bleed rates. This would also result in increased tailpipe temperature and increase in specific thrust. Thus, CDP bleed would be less penalizing for an HSCT engine than fan discharge bleed. This trend was only valid until a maximum allowable T4 was reached. After that point, the penalty for CDP bleed would be very steep since specific thrust and tailpipe mass flow rate are both decreasing.

To summarize, extracting bleed from an HSCT engine did not affect the cycle specific thrust, so the penalty due to 1 lbm/s fan bleed was 98 lb of net thrust. Compressor discharge flow extraction would not decrease specific thrust until the T4 limit was reached. After that point, the penalties for CDP bleed become excessive. A detailed cycle analysis should be performed to determine the exact behavior, but one could conservatively estimate that compressor discharge flow extraction followed the same trend as fan bleed. The maximum allowable CC system mass flow rate was taken to be 240 lbm/s.

An additional factor that was considered was the CC air supply pressure and temperature from the engine. Obviously, high pressures and temperatures allowed smaller mass flow rates and smaller ducting for a given blowing effectiveness. However, the pressure and temperature delivered by the engine depended heavily on the power setting as shown in Table III. Unfortunately, the CC system cannot afford to have large swings in operating pressure, as these would result in a system which was drastically oversized for some flight conditions. The solution to this problem was to use fan bleed air to drive the CC system during takeoff and use CDP bleed during landing. The data of Table III reveals that the bleed pressures during these flight conditions were roughly equal, thus allowing for a nicely tailored CC system. Additionally, compressor discharge air could conceivably be used at takeoff during an emergency, and hence increased lift capability of the wing. Based on these considerations, one could conclude that HSCT engines have sufficient excess capacity to power a CC system even with OEI.

Table III: Pressure and Temperature Variation

	Max Power	Flight Idle
CDP (psia)	266	47
CDT (°R)	1329	787
Fan P (psia)	51	17.1
Fan T (°R)	809	578

The low speed performance metrics were determined based on the same parametric variation conducted on the conventional baseline configuration. In addition to the parameters listed in Table II, the amount of mass flow extracted from each engine was included and allowed to vary between 40 lbm/s and 60 lbm/s. Similar to the baseline parametric investigation of the flap deflections, the application of the CC trends also included deviations on flap deflections to minimize the low speed metrics. Furthermore, the application of the CC trends depended upon the definition of the blowing coefficient, C_μ, as shown in Figure 1. Hence, the mass flow and wing area were defined and an internal duct analysis established the jet velocity as 1,700 ft/s. The only remaining independent variable needed to determine the amount of incremental force coefficients (ΔC_L and ΔC_D) applied was the dynamic pressure (i.e., the vehicle velocity). This dependency on speed created difficulties in the analysis.

As stated previously, TAKEOFF required that an incremental change in lift and drag (ΔC_L or ΔC_D) be represented as a function of vehicle speed for a fixed flap setting and α and which remained constant. The dependency of the force coefficients on speed for the TAKEOFF program assumed that the incremental change of forces coefficients *were constant* with speed. This difficulty in the analysis was due to the internal convergence requirements of the TAKEOFF program. A description of the method of calculation within TAKEOFF was provided so as to establish a means of CC trends application.

The TAKEOFF program began the analysis with the stall speed (V_S). The V_S was determined from the input C_{Lmax}, wing area, and takeoff gross weight. Acceleration tables were established from brake release until $1.5V_S$ for all engine operating (AEO) and OEI. Deceleration tables were then determined from $1.2V_S$ to full stop for AEO and OEI. From these tables, the V_{LOF} was iteratively calculated at the maximum allowable α (i.e., 20º), and the rotation speed (V_R) subsequently determined as the greater of $1.1V_{LOF}$ for AEO or $1.05V_{LOF}$ for OEI. The takeoff profile from rotation to liftoff through the obstacle height with OEI was then determined. At the obstacle height, the speed was by definition V_2. The primary convergence criterion of TAKEOFF was that $V_2=1.2V_S$. If this condition was not met, V_{ROT} was increased.

The convergence problem was more readily understood with a visualization of required and available C_L at the liftoff condition when CC was applied. If one assumes a liftoff angle of attack of 9.8º, the required C_L could be established from a balance of forces, provided a liftoff speed was known. Yet, the available C_L is dependent upon the speed (as shown in Figure 10) due to lift augmentation's dependency on speed. Hence, as ΔC_L and ΔC_D were added, the necessary liftoff speed reduced. This resulted in an instantaneous liftoff of the vehicle which was not physically possible. A temporary solution to this problem was achieved by manually applying the CC effects until the speeds converged for AEO and OEI. One suggestion for future work would be the development of an analysis tool capable of automatically synthesizing an HSCT with CC.

A Design of Experiments was applied to the CC configuration once converged solutions could be obtained. Once again, the low speed metric sensitivities were determined and are displayed in Figure 11. A flap deflection of 10º was found to minimize the low speed metrics. The metric values which resulted were: TOFL of 8,941.5 ft, V_S of 163.3 kts, V_1 of 160.3 kts ,V_R of 190.2 kts, V_{LOF} of 209 kts, and V_2 of 218.2 kts. These metric values were also based on ideal operating conditions (e.g., standard day, maximum capacity).

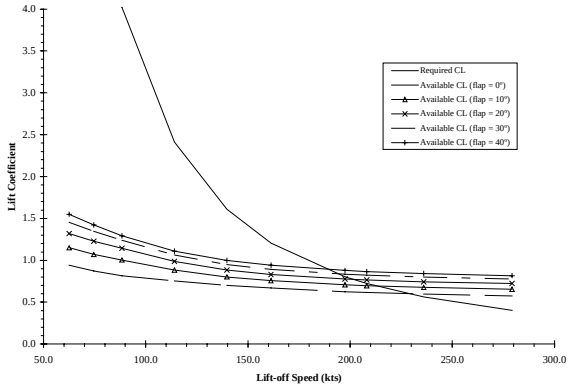

Figure 10: Required C_μ Variation with Lift-off Speed

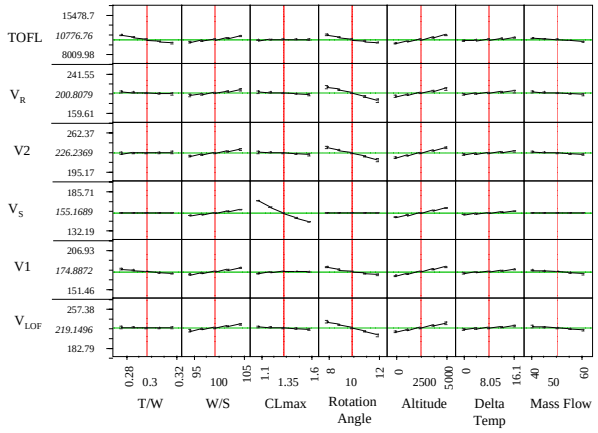

Figure 11: HSCT with 10° CCW Flap

Performance Comparison

The low speed analysis results of the baseline reference configuration and the CC configuration were compared to quantify the differences. Based on the results obtained above for the parametric variations of flaps, the low speed metrics associated with both configurations at standard day conditions are contrasted in Table IV. Both configurations assumed a rotation angle of 9.5º. The CC configuration reduced all metrics, especially, the TOFL which was substantially reduced by 30.1% at standard operating conditions. The reduction in speed magnitudes could be significant in the overall technical feasibility of an HSCT. The application of CC showed improvements in low speed performance, but could also have secondary benefits to other system constraints and should be investigated in future research.

With the maximum capacity reduced, hence the thrust-to-weight and wing loading varied, a carpet plot was obtained as shown in Figure 12. As can be seen, the amount of feasible space for the CC configuration with a 10º flap was much larger. This result implied that the configuration was more robust to off-design conditions. This type of comparison was performed for various altitudes and temperature deviations. The CC configuration consistently out-performed the baseline configuration.

Table IV: Low Speed Metric Comparison at Standard Day Conditions

Metric	Baseline	CC	% Change
TOFL (ft)	12,934	8,941.5	-30.9
V_S (kts)	172.9	163.3	-5.6
V_1 (kts)	186.8	160.3	-14.2
V_R (kts)	221.3	190.2	-14.1
V_{LOF} (kts)	236.1	209	-11.5
V_2 (kts)	241	218.2	-9.5

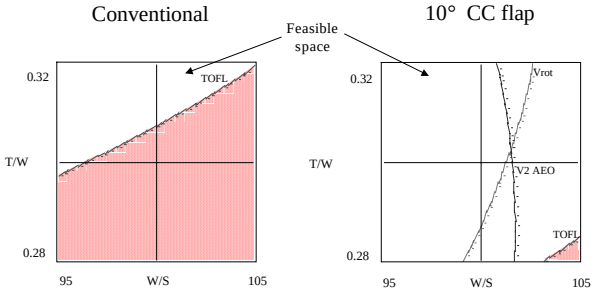

Figure 12: Feasibility Space Comparison at Standard Day Conditions

CONCLUSIONS

In summary, a commercial High Speed Civil Transport was shown not to be technically feasible due to violation of low speed performance constraints, in particular takeoff field length. A conventional configuration could not achieve the 11,000 ft restriction imposed by airport compatibility guidelines. A pneumatic technology, specifically Circulation Control, was suggested as a potential candidate to overcome the constraint violation. Experimental investigations were performed by the Georgia Tech Research Institute to aerodynamically estimate the impact of CC on an HSCT. This study applied the information obtained in those experiments to a computational model. The motivation was to quantify, from a system level point of view, the enhancements and degradations to the to the overall system and the system level constraint, takeoff field length. The impact on the propulsion system was determined to be negligible if bleed air was extracted from the fan.

The wind tunnel data was regressed and applied to a notional HSCT concept, and the low speed metrics assessed. The CC configuration consistently outperformed the conventional configuration for all metrics considered. This study showed that Circulation Control reduced the takeoff field length metric by 31%; reduced the liftoff speed by 11%; and reduced the obstacle height speed by 10%. Not only did the application of CC allowed for the performance constraint to be satisfied, but the speeds associated with airport operations were also reduced.

ACKNOWLEDGMENTS

The authors would like to thank Dr. Jimmy Tai and Mr. Bryce Roth of the Aerospace Systems Design Laboratory for their input and assistance. Also, the research results contained herein were sponsored under NASA Langley grant NAG-1-1517, and the data provided by Mr. Bob Englar of the Georgia Tech Research Institute.

REFERENCES

1. Goldin, D.S., “The Three Pillars of Success for Aviation and Space Transportation in the 21st Century”, speech given before the Aero Club, AIAA, and NAC, March 20, 1997.

2. Mavris, D.N., Kirby, M.R., Qui, S., “Technology Impact Forecasting for a High Speed Civil Transport”, SAE Paper 985547.

3. Ott, J., “HSCT Computer model Takes Shape at NASA”, Aviation Week & Space Technology, Oct 13, 1997, pp 68-69.

4. Kandebo, S.W., “Redefined Propulsion Tests Target HSCT Scale-up Issues”, Aviation Week & Space Technology, Oct 13, 1997, pp 70-72.

5. Kulfan, R.M., “High Speed Civil Transport Opportunities, Challenges and Technology Needs”, Keynote Speech, 34th National Conference on Aeronautics and Astronautics, Tainan, Taiwan, Nov 26, 1992.

6. Hirokawa, J., Sekido, T., Futatsudera, N., “Technologies Required for the Next Generation HSCT, Propulsion Systems”, 7th European Aerospace Conference, Toulouse, France, Oct. 1994.

7. Bunin, B.L., Gray, I.G., Khaski, E., Olszewski, M.W., Schmitt, D., “Second Generation Supersonic: A Case for Global Cooperation”, 7th European Aerospace Conference, Toulouse, France, Oct. 1994.

8. Barbaux, Y., Guedra-Degeorges, D., Lapasset, G., “The Materials Challenge for the Future SCT”, 7th European Aerospace Conference, Toulouse, France, Oct. 1994.

9. Englar, R.J., “Application of Pneumatic Lift and Control Surface Technology to Advanced Transport Aircraft”, presented at *Transportation Beyond 2000: Engineering Design for the Future*, Conference at NASA Langley Research Center, Hampton, Va, Sept 26-28, 1995.

10. Novak, C.J., Cornelius, K.C., Roads, R.K., “Experimental Investigations of the Circular Wall Jet on a Circulation Control Airfoil”, AIAA 87-0155.

11. Englar, R.J., “Investigation into and Application of the High Velocity Circulation Control Wall Jet for High Lift and Drag Generation on STOL Aircraft”, AIAA 74-502.

12. Young, T., “Outlines of Experiments and Inquiries Regarding Sound and Light”, Lecture to the Royal Society, Jan 16, 1800, (see Journal Royal Aeronautical Society, Vol 61, 1957, pp. 157).

13. Kirkpatrick, D.G., Barnes, D.R., “Development and Evolution of the Circulation Control Rotor”, Paper presented at the 36th Annual Forum of the AHS, Washington, D.C., May 1980.

14. Mentral, A., Zerner, F., “The Coanda Effect”, Publication Scientifiques et Technique du Ministere de l’Air”, No 218, 1948.

15. Scrugg, T.B., “Computational Investigation of Circulation Control Turbulence Modeling”, Master’s Thesis, School of Engineering, Air Force Institute of Technology, Dec 1990.

16. Dunham, J., “Circulation Control Applied to Circular Cylinder”, National Gas Turbine Est (England) Report R. 287, July, 1967.

17. Cheeseman, I.C., “Circulation Control and Its Application to Stopped Rotor Aircraft”, AIAA 67-747.

18. Williams, R.M., "Some Research on Rotor Circulation Control", Proc. of the 3rd Cal/AVLABS Symposium, Vol 11, June 1969.
19. Englar, R.J., "Two-Dimensional Transonic Wind Tunnel Tests of Three 15-percent Thick Circulation Control Airfoil", NSRDC Report ASED-182, Dec. 1970.
20. Roberts, S.C., "WVU Circulation Controlled STOL Aircraft Flight Tests", West Virginia University, Morgantown, WV, Aerospace TR-42, July 1974.
21. Pugliese, A.J., Englar, R.J., "Flight Testing the Circulation Controlled Wing", AIAA 79-1791, see also Aviation Week & Space Technology, Mar., 19, 1979.
22. Englar, R.J., "Development of the A-6 Circulation Control Wing Flight Demonstrator Configuration", DTNSRDC/ASED-79/01, Jan. 1979.
23. Harvell, J.K., Franke, M.E., "Aerodynamic Characteristics of a Circulation Controlled Elliptical Airfoil with Blown Jets", AIAA 83-1794.
24. Stevenson, T.A., Franke, M.E., Rhynard, Jr., W.E., Snyder, J.R., "A Wind Tunnel Investigation of a Circulation-Controlled Elliptic Airfoil", AIAA 76-933.
25. Englar, R.J., Smith, M.J., Kelley, S.M., Rover III, R.C., "Development of Circulation Control Technology for Application to Advanced Subsonic Transport Aircraft", AIAA 93-0644.
26. Englar, R.J., Niebur, C.S., Gregory, S.D., "Pneumatic Lift and Control Surface Technology Applied to High Speed Civil Transport Configurations", AIAA 97-0036.
27. McCullers, L.A., *Detailed Takeoff and Landing Analysis Program User's Guide, Version 2.0*, NASA Langley Research Center, Hampton, Va., June 20, 1994.
28. McCullers, L.A., *FLOPS User's Guide, Version 5.94*, NASA Langley Research Center, Hampton, Va., Jan 16, 1998.
29. Mavris, D.N., Mantis, G.C., Kirby, M.R., "Demonstration of a Probabilistic Technique for the Determination of Aircraft Economic Viability", SAE Technical Paper 97-5585.
30. Kirby, M.R., Mavris, D.N., "Forecasting the Impact of Technology Infusion on Subsonic Transport Affordability", SAE Technical Paper 98-5576.
31. SAS Institute Inc., *JMP, Computer Program and Users Manual*, Cary, NC, 1994.
32. Carlson, H.W., Chu, J., Ozoroski, L.P., McCullers, L.A., "Guide to AERO2S and WINGDES Computer Codes for Prediction and Minimization of Drag Due to Lift", NASA TP-3637, 1997.
33. Box, G.E.P., Hunter, W.G., Hunter, J.S., Statistics for Experimenters, An Introduction to Design, Analysis, and Model Building, John Wiley & Sons, New York, 1978.